Please cite the Published Version

Additional Information: This is an Author Accepted Manuscript of a paper accepted for publication in Nature Nanotechnology, published by and copyright Nature Research.

Non-precious metal hydrogen catalyst in commercial polymer electrolyte membrane electrolysers

Authors:

Laurie A. King,[1][¥] McKenzie A. Hubert,[1][¥] Christopher Capuano,[2] Judith Manco,[2] Nemanja Danilovic,[3] Eduardo Valle,[1] Thomas R. Hellstern[1], Katherine Ayers,[2] and Thomas F. Jaramillo*[1]

Affiliations:

[1] Department of Chemical Engineering, Shriram Center, Stanford University, 443 Via Ortega, Stanford, CA 94305, USA

[2] Nel Hydrogen/Proton OnSite, 10 Technology Drive, Wallingford, CT 06492, USA

[3] Lawrence Berkeley National Lab, 1 Cyclotron Road, Berkeley, CA 94720, USA

*Corresponding author: jaramillo@stanford.edu

Abstract:

We demonstrate the translation of a low cost, non-precious metal cobalt phosphide (CoP) catalyst from 1 cm^2 lab-scale experiments to a commercial-scale 86 cm^2 polymer electrolyte membrane (PEM) electrolyser. A 2-step bulk synthesis was adopted to produce CoP on a high surface area carbon support that was readily integrated into an industrial PEM electrolyser fabrication process. The performance of the CoP was compared head-to-head with a platinum-based PEM under the same operating conditions (400 psi, 50 °C). CoP was found to be active and stable, operating at 1.86 $A.cm^{-2}$ for >1700 hours of continuous hydrogen production while providing substantial material cost savings relative to platinum. This work illustrates a potential pathway for non-precious hydrogen evolution catalysts developed in past decades to translate to commercial applications.

Main Text:

The modern-day commercialisation of large-scale polymer electrolyte membrane (PEM) water electrolysers represents the culmination of decades of fundamental scientific studies involving catalysts, membranes, electrode architectures, and membrane electrode assemblies (MEAs) among other key advancements. Commercial PEM electrolysers utilize expensive platinum group catalysts such as platinum and iridium, despite their high costs and scarcity, to achieve and maintain high activity over 50,000 h. Terawatt-scale deployment of electrolysers envisioned for grid resilience require significant reduction of platinum group catalysts and/or replacement by alternative non-platinum group (NPG) catalysts within the device (*1*). This goal presents many challenges, including the need to tailor catalyst inks, tune deposition methods, and provide stable activity at elevated temperatures, pressures, and current densities, all while demonstrating high activity and durability over the lifetime expected of a commercial system. In this study, we bridge the gap between decades of lab-scale, solution-based, NPG catalyst development and industrial-scale electrolyser operation. We report the first integration of a highly active NPG catalyst (cobalt phosphide, CoP) into a commercial grade PEM electrolyser with >1700 hours of continuous operation and negligible loss in activity. We briefly discuss the economic trade-off of replacing the traditional Pt cathode with a NPG catalyst while emphasizing the promise of NPG materials to supersede precious metal catalysts in commercial PEM electrolysers.

Recent technoeconomic analyses suggest that PEM electrolysis is a promising technology for widespread renewable hydrogen production, hinging on capital cost reductions that would make this technology competitive in the hydrogen market (*1*). Overcoming this challenge requires cost reductions across many system components, demanding substantial innovation in material design, engineering, and manufacturing. Reducing precious metal content has been a major R&D effort among manufacturers of PEM electrolysers, as doing so would reduce capital costs while also mitigating issues of material scarcity. While Pt and Ir catalysts constitute ~8% of the total stack cost today, price inelasticity, and therefore volatility, of these precious metals hinder future TW-scale deployment of PEM electrolysis (*2*). This motivates the development of active and stable NPG hydrogen evolution reaction (HER) catalysts, the best-case scenario for reducing Pt content in PEM electrolysers.

62 Inspired by hydrogen-producing enzymes such as nitrogenase, molybdenum disulphide

63 (MoS$_2$) emerged as one of the first promising NPG HER catalysts (*3*, *4*). Subsequently,

64 researchers pursued similar classes of materials, including transition metal phosphides,

65 which exhibit favourable activities and stabilities in lab scale demonstrations (*5–7*).

66 Significant advances in the activities of NPG catalysts have been accomplished by tuning

67 the morphology, chemical composition, and crystal structure via synthesis methods (*5*,

68 *6*). Universal to nearly all published NPG HER literature are the electrochemical testing

69 protocols used to measure catalyst activity and stability (linear sweep voltammetry,

70 cyclic voltammetry, chronoamperometry, and/or chronopotentiometry) (*8*). Such

71 methodologies provide figures of merits such as onset potential, exchange current

72 densities, and Tafel slopes which enable benchmarking, as well as provide insightful

73 fundamental knowledge. However, relatively few studies have translated NPG catalysts

74 to PEM electrolyser devices (*9–12*) and to the best of our knowledge, there are no reports

75 demonstrating their integration in commercial-scale systems at relevant sizes, current

76 densities, pressures, and temperatures.

77

78 Herein, we report the first translation of a NPG HER catalyst into a commercial-scale PEM

79 electrolyser. Thanks to the development efforts of many, there were a multitude of

80 potential NPG catalyst candidates (*5*, *13*, *14*). For this first demonstration we selected

81 CoP, as experimental and theoretical studies have shown it to have promising HER

82 activity in the acidic environments relevant for PEM electrolysers (*15–19*). The CoP was

83 prepared by wetness impregnation of cobalt nitrate onto Vulcan carbon followed by

84 vapour phase phosphidation. The phosphidation step was adapted from a previous

85 report wherein a CoP thin film was fabricated on a silicon substrate (*18*). The direct

86 growth of the phosphide on the carbon support facilitates mechanical adhesion of the

87 catalyst to the substrate and enhances uniform electrical conductivity and dispersion of

88 the catalyst (*6*). Our simple 2-step synthesis produced >1.1 gram powder catalyst batch

89 sizes, amenable to MEA fabrication using ink-based methods. This method has the

90 potential for orders of magnitude scale-up, as batch size was only limited by the reactor

91 size employed. Synthetic details are provided in the supplementary information.

92

93 Shown in Fig. 1A is the X-ray diffraction (XRD) pattern of the as-synthesised catalyst,

94 confirming that our developed method generates a phase-pure catalyst (FeAs-type CoP).

95   X-ray photoelectron spectroscopy (XPS) of the as-prepared catalyst shows the presence

96   of CoP, cobalt oxide, and phosphate species (Fig. S1), which are commonly reported for

97   CoP (*20*). The loading of CoP on the Vulcan carbon support was ~21wt% with a Co:P

98   molar ratio of 1:1, determined using inductively coupled plasma mass spectrometry (ICP-

99   MS) (Tables S1 and S2).

100
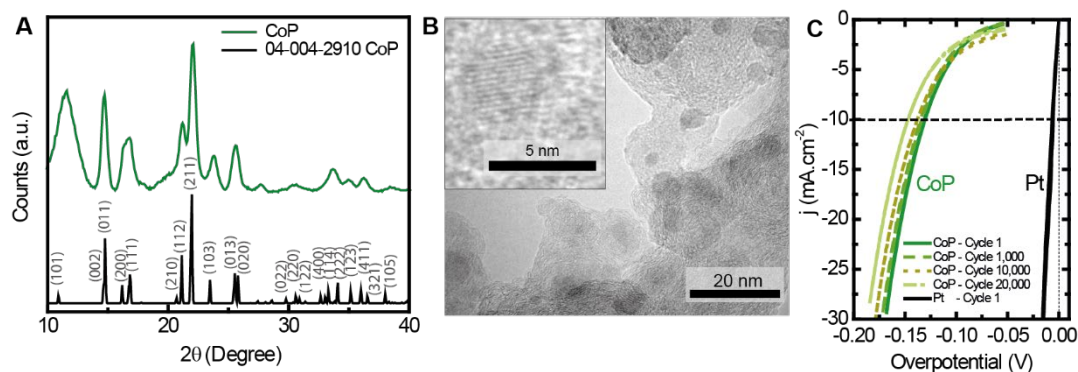
Fig. 1. Physical and electrochemical characterisation of the CoP catalyst. (A)
Powder XRD. (B) TEM micrograph. Inset shows a higher magnification micrograph of a
CoP nanoparticle. (C) Linear sweep voltammograms (LSVs) (iR-corrected) of the CoP
catalyst (0.12 $mg_{CoP}.cm^{-2}$) and commercial Pt catalyst (0.12 $mg_{Pt}.cm^{-2}$) drop cast onto
carbon paper and tested in a 3-electrode electrochemical cell in 0.5 M H_2SO_4. LSVs are
shown for the as-prepared CoP and commercial Pt (cycle 1), as well as after 1,000, 10,000
and 20,000 cycles of accelerated cyclic voltammograms for the CoP catalyst.

108

109   The morphology of the catalyst was examined with transmission electron microscopy

110   (TEM) and scanning electron microscopy (SEM) (Fig. 1B and Fig. S2). TEM enables clear

111   identification of CoP nanoparticles with an average diameter of ~5 nm (Fig. 1B). HR-TEM

112   (Fig. 1B inset) confirms lattice plane spacing of 2.5 Å which matches FeAs-type CoP (111)

113   (*16*). Lower magnification TEM micrographs show that CoP is well-dispersed on the

114   Vulcan carbon support (Fig. S3). Thus, we report a facile synthesis route, consisting of

115   simple precursors and few processing steps, which yields a high surface area

116   nanoparticulate CoP catalyst that is amenable to scaled-up MEA fabrication requiring

117   minimal technical changes.

118   Lab-scale measurements, in acidic electrolyte (Fig. 1C) revealed excellent activity and

119   stability of the CoP catalyst (Fig. S4 and Fig. S5), in-line with previous studies (*21*, *22*).

120   For comparison, the activity of a commercial Pt catalyst of similar loading is also shown

121   (Fig. 1C). While the activity of the CoP catalyst does not rival that of Pt, CoP showed little

122 degradation under lab-scale cyclic voltammetry durability testing conditions and
123 reasonable onset potentials. It is well known that 3-electrode stability measurements do
124 not necessarily translate into MEA stability (*23–25*), which motivated further
125 examination of the CoP catalyst in a MEA. Although CoP is not the most active catalyst in
126 the literature (*5*), it represents a platform for performing these initial and important
127 feasibility screenings of NPG catalysts within a commercial-grade electrolyser,
128 motivating exploration of other NPG catalysts within these systems.

129 To fabricate cathode gas diffusion electrodes (GDEs), the catalyst was dispersed in a
130 suspension of Nafion ionomer, IPA, and water, then spray coated onto carbon paper gas
131 diffusion layers. The anode GDE used IrO_x as the baseline material, a known durable
132 catalyst, which isolated any observed performance changes in the electrolyser to the NPG
133 cathode. A Nafion 117 proton exchange membrane was used in the MEA, placed between
134 the anode and cathode GDEs. The MEAs were assembled in Proton OnSite's commercial
135 86 cm^2 active area PEM-electrolyser cell stack (Fig. 2A) along with a baseline all-PGM cell
136 (Pt black-based GDE) for direct comparison under identical operating conditions. All
137 tests were conducted at 400 psi hydrogen differential pressure and at elevated
138 temperatures with liquid water fed to the anode side of the cell. Table S3 highlights the
139 distinct differences between the 3-electrode lab-scale setup and the commercial-grade
140 testing protocol.

141 The CoP catalyst was loaded at 1.0 $mg_{CoP}.cm^{-2}$ on the GDE, equivalent to 4.5 $mg.cm^{-2}$ total
142 catalyst loading including the carbon support. The electrolyser was first characterised
143 by stepping the current from 100 $mA.cm^{-2}$ (1.54V) to 1.86 $A.cm^{-2}$ (2.27 V) at 50 °C (Fig.
144 2B). Interestingly, the polarisation curve shows this non-precious catalyst can reach the
145 same high current densities as the Pt-containing cell at reasonable potentials. Assuming
146 that every unit of CoP is active for the HER, a conservative estimate for the turnover
147 frequency (TOF) of CoP is 0.87 $H_2.s^{-1}$. More likely, only the surface bound CoP units (~10
148 %) participate in the reaction, leading to an estimated TOF_{avg} of 8.7 $H_2.s^{-1}$. Comparatively,
149 the TOF for the Pt catalyst is estimated to be 1.88 $H_2.s^{-1}$ conservatively, or 28.8 $H_2.s^{-1}$
150 assuming only surface atoms participate in the reaction. Details of the calculations are
151 shown in the supplementary information.

152 The all-PGM baseline GDE shows that the Pt PEM required 2.05 V to reach a current
153 density of 1.86 $A.cm^{-2}$ (Fig. 2B). This result reflects operating efficiencies of 55% and 61%

respectively for the CoP- and Pt-based electrolysers based on the lower heating value
(LHV). While the fact that the Pt system performs 220 mV better than the NPG catalyst is
not surprising given the 3-electrode measurements (Fig. 1C), this small difference is
impressive considering the commercially relevant high current densities employed.
Future work will explore electrode engineering to maximize the performance of NPG
based electrolysers. Optimization of catalyst loading and ionomer content, for example,
will only help to narrow the performance gap between PGM and NPG catalysts in
commercial electrolyser platforms. This gap will continue to shrink as NPG catalysts
themselves are further improved, minimizing the trade-offs between operating and
capital costs (*14*).
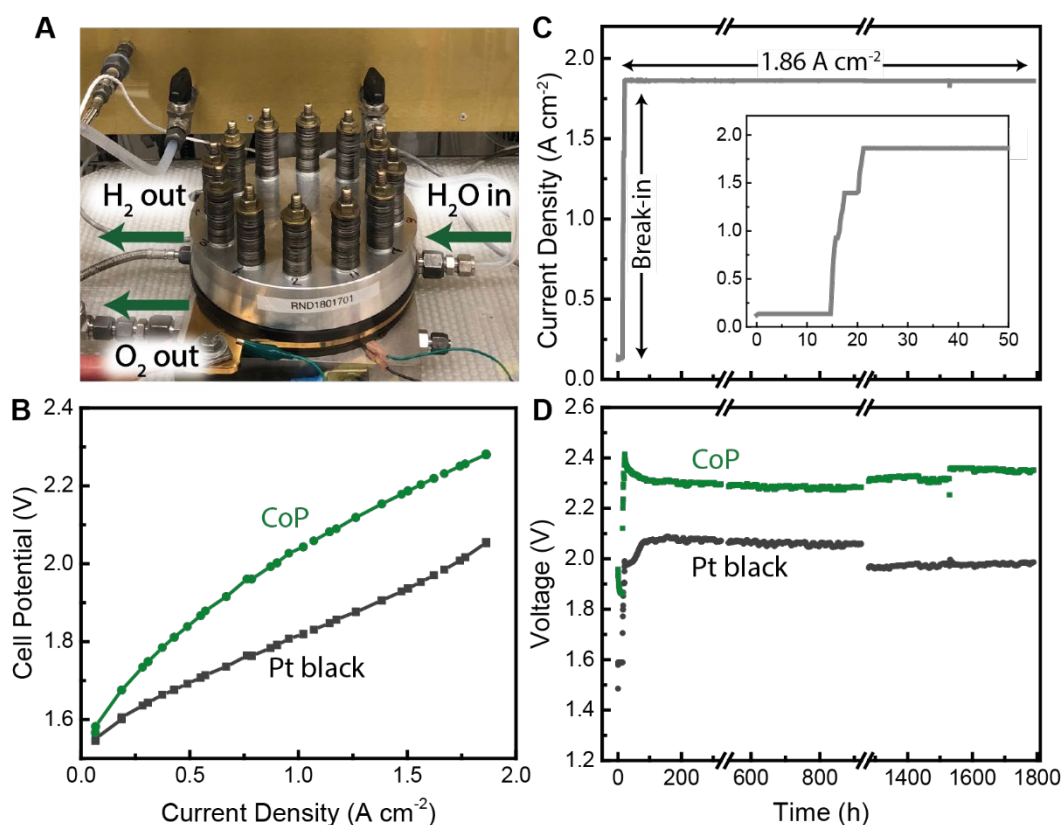
Fig. 2. PEM electrolyser performance. (A) Photograph of the 86 cm^2 electrolyser test
station. (B) Polarisation curve. (C) Current density profile for the durability protocol.
The inset shows the current density profile for the break-in period only. (D) Durability
voltage-time plots for the PEM electrolyser prepared with 1.0 mg$_{CoP}$.cm^{-2} loading while
operating at 50 °C and 400 psi. Voltage discontinuities result from power outage-induced
restarts.

The CoP and Pt-based MEA durability tests were also conducted in the 2-cell stack following the polarisation studies. The differences in operating conditions between the 2-electrode and 3-electrode stability measurements are noted in Table S3. The tests were initiated at 50 °C and held at 0.135 A.cm^{-2} for $\sim$20 h (Fig. 2C and 2D). After 20 h of operation, the temperature was ramped to 55 °C and the current was increased to 1.86 A.cm^{-2} over 6 h. The current density was subsequently held at 1.86 A.cm^{-2} for the remaining 1763 h of testing. During the durability measurement, the CoP MEA stabilised within 50 h to provide steady operation at 2.30 V for >900 h with energy consumption of 60.4 kWh.kg$_{H2}$$^{-1}$. The Pt-based MEA operated under the same conditions (1.86 A.cm^{-2}, 55 °C, 400 psi) at 2.06 V as expected without degradation, corresponding to energy consumption of 54.5 kWh.kg$_{H2}$$^{-1}$. Transient behaviour in the break-in phase is discussed in the supplementary information.

After 922 h of continuous testing, the 2-cell stack (CoP and Pt MEAs) lost power briefly (<1 min) and was restarted. The reset resulted in an increase ($\sim$50 mV) in cell potential for the CoP MEA and a slightly reduced potential for the Pt MEA ($\sim$6 mV). A second, small abrupt increase in potential was observed after 1550 h of operation, likely due to a second disruption in the applied potential. Duplicate CoP and Pt MEAs were fabricated and tested with a similar protocol and were shown to be extremely stable with comparable cell potentials (Fig. S6). Discussion of the MEA restarts and characterisation of the CoP GDE after the 1700 h durability test are provided in the supplementary information (Fig. S7). Analogous to the fuel cell literature, it is important to note that Pt-based commercial PEM electrolysers are also known to degrade on start-up and shut-down cycling and hence this challenge is relevant for all known catalysts, precious metal and non-PGMs alike (26).

In a 3-electrode lab-scale configuration, it has been reported that non-precious metal ionic compound catalysts such as transition metal phosphides dissolve at higher rates under OCP conditions, but are stable when evolving hydrogen, even when cycling from low to high production rates (27, 28). This report is consistent with our lab-scale durability measurements of CoP dissolution during electrochemical testing (Fig. S8 and Fig. S9). We therefore postulate that CoP dissolution occurred when the MEA lost power briefly after 922 h and 1550 h of operation leading to the increased cell potential.

203   Furthermore, we propose operating procedures that maintain a small operating current

204   could prevent this degradation mechanism.

205   Remarkably, the CoP MEA produced a total of 10.1 kg of H_2 (912 L at STP), and we

206   conservatively estimate a turnover number (TON) of 5.3 x 10^6 H_2 molecules produced per

207   CoP site assuming all CoP units are active. Details of the calculations are shown in the

208   supplementary information. The CoP MEA requires 12 – 18 % greater power density

209   than the Pt baseline MEA, a potentially attractive trade-off between electricity

210   consumption and electrolyser capital cost depending on the application and the local cost

211   of electricity. While this work highlights a significant step towards non-PGM catalyst

212   incorporation in commercial electrolysers, the difference in performance between CoP

213   and Pt is still too substantial for wide-scale commercial deployment, motivating

214   continued research and development of non-PGM catalysts.

215   Analyses show that the levelized cost of hydrogen (LCH) from water electrolysis is

216   currently dominated by the cost of electricity (*29*, *30*). However, as society follows a path

217   towards increased electrification and electricity prices drop, the capital cost of

218   electrolysers will begin to dominate (*31*, *32*). Utilisation of durable, low-cost NPG

219   catalysts that can replace expensive and price inelastic precious metals is one critical step

220   towards reducing the overall capital cost of PEM electrolysis (Table S4). While the result

221   presented here is a significant achievement, we note that cost reductions across all

222   system components are needed for TW-scale deployment of PEM electrolysers. A full

223   techno-economic analysis on the implications of this report is outside the scope and will

224   be the subject of future investigations.

225   Our initial demonstration of an active and highly stable NPG HER catalyst in a

226   commercial-scale PEM electrolyser highlights the practical relevance of NPG systems. By

227   extending our lab-scale stability study from liquid electrolyte and 1 cm^2 electrode area to

228   an 86 cm^2 commercial PEM electrolyser with >1700 h of stable operation at elevated

229   temperature and pressure, we demonstrate the commercial relevance of NPG catalysts.

230   Compared to a Pt-based PEM, we found the CoP PEM to pay a 12 – 18 % power penalty

231   under the operating conditions, but to provide a significant improvement in material cost

232   over the commercial Pt catalyst. We believe that the results represent a possible entry

233   point for NPG catalyst utilisation in commercial water electrolysers. Continued research

234   efforts between industry and academia enables pathways to lowering the capital

235 investment costs of PEM electrolysers while maintaining high operating efficiencies to
236 implement grid-scale energy storage.

Methods

237 Methods, including statements of data availability are available in the Supplementary
239 Information.

240

References and Notes

242 1. L. Bertuccioli *et al.*, Study on development of water electrolysis in the EU. *Fuel Cells*
243 *Hydrog. Jt. Undert.*, 1–160 (2014).

244 2. P. C. K. Vesborg, T. F. Jaramillo, Addressing the terawatt challenge: scalability in the
245 supply of chemical elements for renewable energy. *RSC Adv.* **2**, 7933 (2012).

246 3. B. Hinnemann *et al.*, Biomimetic Hydrogen Evolution: MoS2 Nanoparticles as Catalyst for
247 Hydrogen Evolution. *J Am Chem Soc*. **36**, 5308–5309 (2005).

248 4. T. F. Jaramillo *et al.*, Identification of Active Edge Sites for Electrochemical H2 Evolution
249 from MoS2 Nanocatalysts. *Science (80-.).* **317**, 100–102 (2007).

250 5. J. F. Callejas, C. G. Read, C. W. Roske, N. S. Lewis, R. E. Schaak, Synthesis , Characterization ,
251 and Properties of Metal Phosphide Catalysts for the Hydrogen-Evolution Reaction. *Chem.*
252 *Mater.* (2016), doi:10.1021/acs.chemmater.6b02148.

253 6. Y. Shi, B. Zhang, Recent advances in transition metal phosphide nanomaterials: synthesis
254 and applications in hydrogen evolution reaction. *Chem. Soc. Rev.* **45**, 1529–1541 (2016).

255 7. J. Kibsgaard, T. F. Jaramillo, Molybdenum phosphosulfide: An active, acid-stable, earth-
256 Abundant catalyst for the hydrogen evolution reaction. *Angew. Chemie - Int. Ed.* **53**,
257 14433–14437 (2014).

258 8. C. C. L. McCrory *et al.*, Benchmarking Hydrogen Evolving Reaction and Oxygen Evolving
259 Reaction Electrocatalysts for Solar Water Splitting Devices. *J. Am. Chem. Soc.* **137**, 4347–
260 4357 (2015).

261 9. T. Corrales-Sánchez, J. Ampurdanés, A. Urakawa, MoS2-based materials as alternative
262 cathode catalyst for PEM electrolysis. *Int. J. Hydrogen Energy*. **39**, 20837–20843 (2014).

263 10. J. W. D. Ng *et al.*, Polymer Electrolyte Membrane Electrolyzers Utilizing Non-precious Mo-
264 based Hydrogen Evolution Catalysts. *ChemSusChem*. **8**, 3512–3519 (2015).

265 11. C. Di Giovanni *et al.*, Low-Cost Nanostructured Iron Sulfide Electrocatalysts for PEM
266 Water Electrolysis. *ACS Catal.* **6**, 2626–2631 (2016).

267 12. X. Sun *et al.*, Earth-Abundant Electrocatalysts in Proton Exchange Membrane
268 Electrolyzers. *Catalysts*. **8**, 657 (2018).

269 13. S. Anantharaj *et al.*, Recent Trends and Perspectives in Electrochemical Water Splitting
270 with an Emphasis on Sulfide, Selenide, and Phosphide Catalysts of Fe, Co, and Ni: A
271 Review. *ACS Catal.* **6**, 8069–8097 (2016).

272 14. P. Xiao, W. Chen, X. Wang, A Review of Phosphide-Based Materials for Electrocatalytic

273   Hydrogen Evolution. *Adv. Energy Mater.* **5**, 1–13 (2015).

274 15. W. Liu *et al.*, A highly active and stable hydrogen evolution catalyst based on pyrite-
275   structured cobalt phosphosulfide. *Nat. Commun.* **7**, 1–9 (2016).

276 16. E. J. Popczun, C. G. Read, C. W. Roske, N. S. Lewis, R. E. Schaak, Highly Active
277   Electrocatalysis of the Hydrogen Evolution Reaction by Cobalt Phosphide Nanoparticles
278   ** Angewandte. *Angew. Chemie - Int. Ed.*, 5531–5534 (2014).

279 17. J. Kibsgaard *et al.*, Designing an improved transition metal phosphide catalyst for
280   hydrogen evolution using experimental and theoretical trends. *Energy Environ. Sci.* **8**,
281   3022–3029 (2015).

282 18. T. R. Hellstern, J. D. Benck, J. Kibsgaard, C. Hahn, T. F. Jaramillo, Engineering Cobalt
283   Phosphide (CoP) Thin Film Catalysts for Enhanced Hydrogen Evolution Activity on
284   Silicon Photocathodes. *Adv. Energy Mater.* (2016), doi:10.1002/aenm.201501758.

285 19. Z. Wu, L. Huang, H. Liu, H. Wang, Element-Specific Restructuring of Anion- and Cation-
286   Substituted Cobalt Phosphide Nanoparticles under Electrochemical Water-Splitting
287   Conditions. *ACS Catal.* **9**, 2956–2961 (2019).

288 20. F. H. Saadi *et al.*, Operando Spectroscopic Analysis of CoP Films Electrocatalyzing the
289   Hydrogen-Evolution Reaction. *J. Am. Chem. Soc.* **139**, 12927–12930 (2017).

290 21. H. Yang, Y. Zhang, F. Hu, Q. Wang, Urchin-like CoP Nanocrystals as Hydrogen Evolution
291   Reaction and Oxygen Reduction Reaction Dual-Electrocatalyst with Superior Stability.
292   *Nano Lett.* **15**, 7616–7620 (2015).

293 22. D. Zhou *et al.*, Interconnected urchin-like cobalt phosphide microspheres film for highly
294   efficient electrochemical hydrogen evolution in both acidic and basic media. *J. Mater.*
295   *Chem. A.* **4**, 10114–10117 (2016).

296 23. S. Martens *et al.*, A comparison of rotating disc electrode, floating electrode technique and
297   membrane electrode assembly measurements for catalyst testing. *J. Power Sources*. **392**,
298   274–284 (2018).

299 24. S. M. Alia *et al.*, Activity and Durability of Iridium Nanoparticles in the Oxygen Evolution
300   Reaction. *J. Electrochem. Soc.* **163**, F3105–F3112 (2016).

301 25. S. M. Alia, B. S. Pivovar, Iridium-Based Nanowires as Highly Active, Oxygen Evolution
302   Reaction Electrocatalysts. *ACS Catal.* **8**, 2111–2120 (2018).

303 26. A. Weiß, A. Siebel, M. Bernt, H. A. Gasteiger, Impact of Intermittent Operation on the
304   Lifetime and Performance of a PEM Water Electrolyzer. *Meet. Abstr.* . **MA2018**-**02**, 1606
305   (2018).

306 27. Y. Zhang, L. Gao, E. J. M. Hensen, J. P. Hofmann, Evaluating the Stability of Co 2 P
307   Electrocatalysts in the Hydrogen Evolution Reaction for Both Acidic and Alkaline
308   Electrolytes. *ACS Energy Lett.*, 1360–1365 (2018).

309 28. M. Ledendecker *et al.*, Stability and Activity of Non-Noble-Metal-Based Catalysts Toward
310   the Hydrogen Evolution Reaction. *Angew. Chemie*. **129**, 9899–9903 (2017).

311 29. B. James, W. Colella, J. Moton, G. Saur, T. Ramsden, PEM Electrolysis H2A Production Case
312   Study Documentation. *PEM Electrolysis H2A Prod. Case Study Doc.*, 1–27 (2013).

313 30. U. Babic, M. Suermann, F. N. Büchi, L. Gubler, T. J. Schmidt, Critical Review—Identifying
314   Critical Gaps for Polymer Electrolyte Water Electrolysis Development. *J. Electrochem. Soc.*
315   **164**, F387–F399 (2017).

316 31. I. Introduction, Introduction - DOE 2013 Hydrogen and Fuel Cells Program Annual
317   Progress Report (2017).

318 32. F. Cell, T. Office, N. Renewable, 2017 H2 @ Scale Workshop Report (2017).

319

332

333 **Authors contributions:** L.A.K. and M.A.H. contributed equally to this work. L.A.K., M.A.H.,

334 and T.R.H. synthesized CoP catalysts. L.A.K. performed x-ray diffraction and scanning

335 electron microscopy characterisation. E.V. performed transmission electron microscopy

336 characterisation. M.A.H. performed electrochemical lab-scale characterisation and

337 testing. C.C., J.M., and N.D. prepared all PEM stack components, assembled and tested the

338 electrolyser, as well as collected all operational data. L.A.K. and M.A.H. contributed to

339 data analysis, including preparation and revision of this manuscript.

340

341 **Competing interests:** None.

342

343 **Data and materials availability:** The x-ray diffraction reference pattern is available

344 from the Materials Project database under the ID mp-22270. Full synthetic details,

345 electrochemical testing protocols, and raw data can be found in the supplementary

346 information section.

347

348 **Supplementary Information**

349 Materials and Methods
350 Figures S1 – S9
351 Table S1 – S4
352 Turnover frequency and turnover number estimations
353 Electrolyser efficiency calculations
354